

Sphingosine-1-Phosphate Lyase Inhibition Alters the S1P Gradient and Ameliorates Crohn's-Like Ileitis by Suppressing Thymocyte Maturation

Thangaraj Karuppuchamy, PhD,^{*,†} Christopher J. Tyler, PhD,^{*,†} Luke R. Lundborg,^{*,†} Tamara Pérez-Jeldres, MD,^{‡,§} Abigail K. Kimball,^{¶,||} Eric T. Clambey, PhD,^{¶,||} Paul Jedlicka, MD, PhD,^{**} and Jesús Rivera-Nieves, MD^{*,†}

Background: Lymphocytes recirculate from tissues to blood following the sphingosine-1-phosphate (S1P) gradient (low in tissues, high in blood), maintained by synthetic and degradative enzymes, among which the S1P lyase (SPL) irreversibly degrades S1P. The role of SPL in the intestine, both during homeostasis and IBD, is poorly understood. We hypothesized that modulation of tissue S1P levels might be advantageous over S1P receptor (S1PR) agonists (eg, fingolimod, ozanimod, etrasimod), as without S1PR engagement there might be less likelihood of potential off-target effects.

Methods: First we examined SPL mRNA transcripts and SPL localization in tissues by quantitative reverse transcription polymerase chain reaction and immunohistochemistry. The *in vivo* effects of the SPL inhibitors 4-deoxyripyridoxine hydrochloride (30 mg/L) and 2-acetyl-4 (tetrahydroxybutyl)imidazole (50 mg/L) were assessed through their oral administration to adult TNFΔARE mice, which spontaneously develop Crohn's-like chronic ileitis. The effect of SPL inhibition on circulating and tissue lymphocytes, transcriptional regulation of proinflammatory cytokines, and on the histological severity of ileitis was additionally examined. Tissue S1P levels were determined by liquid chromatography–mass spectrometry. Mechanistically, the potential effects of high S1P tissue levels on intestinal leukocyte apoptosis were assessed via terminal deoxynucleotidyl transferase dUTP nick end-labeling assay and annexin 5 staining. Finally, we examined the ability of T cells to home to the intestine, along with the effects of SPL inhibition on cellular subsets within immune compartments via flow and mass cytometry.

Results: S1P lyase was ubiquitously expressed. In the gut, immunohistochemistry predominantly localized it to small intestinal epithelia, although the lamina propria leukocyte fraction had higher mRNA transcripts. Inhibition of SPL markedly increased local intestinal S1P levels, induced peripheral lymphopenia, downregulated proinflammatory cytokines, and attenuated chronic ileitis in mice. SPL inhibition reduced T and myeloid cells in secondary lymphoid tissues and the intestine and decreased naïve T-cell recruitment. The anti-inflammatory activity of SPL inhibition was not mediated by leukocyte apoptosis, nor by interference with the homing of lymphocytes to the intestine, and was independent of its peripheral lymphopenic effect. However, SPL inhibition promoted thymic atrophy and depleted late immature T cells (CD4+CD8+ double positive), with accumulation of mature CD4+CD8- and CD4-CD8+ single-positive cells.

Conclusions: Inhibition of the S1P lyase alters the S1P gradient and attenuates chronic ileitis via central immunosuppression. SPL inhibition could represent a potential way to tame an overactive immune response during IBD and other T-cell-mediated chronic inflammatory diseases.

Key Words: S1P gradient, inflammatory bowel disease, T cells, thymic atrophy

INTRODUCTION

Interference with lymphocyte trafficking is a proven therapeutic strategy for inflammatory bowel disease (IBD),¹ and antibodies against $\alpha 4$ integrins (natalizumab)² and $\alpha 4\beta 7$ (vedolizumab)³ are Food and Drug Administration approved for the treatment of Crohn's and ulcerative colitis. Limitations of antibody-based therapies include high production cost, parenteral administration, risk of infection/cancer,⁴ and development of antidrug antibodies, with subsequent loss of clinical response (secondary failure). These have led to the testing of a newer class of orally administered small molecules that target sphingosine-1-phosphate (S1P) receptors (S1PR agonists), with the prototype drug (ie, fingolimod) approved for the treatment of multiple sclerosis.

S1P is a bioactive sphingolipid that signals through 5G-protein-coupled receptors (GPCRs: S1PR1-5)⁵⁻⁷ and is a critical regulator of many pathophysiological processes (cell adhesion, migration, proliferation, differentiation, and survival).⁸ Ozanimod, a small molecule agonist that targets S1P receptors

Received for publications March 18, 2019; Editorial Decision July 4, 2019.

From the *Inflammatory Bowel Disease Center, Division of Gastroenterology, University of California San Diego, La Jolla, California, USA; †Gastroenterology Section, San Diego VA Medical Center, La Jolla Village Drive, San Diego, California, USA; ‡Universidad Católica de Chile, Santiago, Chile; §Hospital San Borja Arriarán, Santiago, Chile; Departments of ¶Anesthesiology and ¶Pathology, **Department of Pathology, University of Colorado, Anschutz Medical Campus, Aurora, Colorado, USA

Supported by: Funded by a grant from the National Institutes of Health (NIDDK108670) and the BLRD VA Merit Review award (1101BX003436).

Conflicts of interest: The authors disclose no conflicts.

Author contributions: J.R.N. supervised the overall project. T.K. and J.R.N. designed the experiments and wrote the manuscript. T.K. performed most of the experiments with assistance from J.B., L.R.B., C.J.T., L.G., T.P.J. A.K.K., E.T.C., and P.J. assisted with analysis of the data. All authors contributed to the interpretation of the data and proofreading the manuscript.

Address correspondence to: Jesús Rivera-Nieves, MD, Inflammatory Bowel Disease Center, Division of Gastroenterology, University of California San Diego, 9500 Gilman Drive, Bldg. BRF-II, Rm. 4A32, San Diego, CA 92093-0063 (jriveranieves@ucsd.edu).

© 2019 Crohn's & Colitis Foundation. Published by Oxford University Press. All rights reserved. For permissions, please e-mail: journals.permissions@oup.com.

doi: 10.1093/ibd/izz174

Published online 6 December 2019

1 and 5, met all clinical trial end points in patients with moderate to severe ulcerative colitis (UC).⁹ Similarly, etrasimod, which targets SIP receptors 1, 4, and 5, has also shown preliminary efficacy and safety. SIPR agonists act as functional antagonists, which upon engagement polyubiquitinate¹⁰ receptors, leading to their proteasomal degradation. This desensitizes lymphocytes, rendering them unable to sense SIP and recirculate.¹¹

SIP levels are tightly regulated by synthetic and degradative enzymes, which maintain low SIP levels in tissues through the action of the SIP lyase (SPL) and 2 phosphatases (Supplementary Fig. 1A).¹² By contrast, SIP is high in blood, where SPL is not expressed. This difference constitutes the SIP gradient, which regulates lymphocyte recirculation and maintains vascular integrity and lymphatic endothelial barrier function.^{7, 13, 14} However, as SIPRs signal and mediate numerous physiologic functions, we hypothesized that modulation of local SIP levels (without receptor engagement) might be advantageous over SIPR agonists, which engage critical receptors, leading to potential off-target effects.^{15, 16}

Several inhibitors of the SPL have been described,¹⁷ particularly, 2-acetyl-4 (tetrahydroxybutyl)imidazole (THI), which was found to be safe in phase 2 trials, and the vitamin B₆ antagonist 4-deoxyribose (DOP), which inhibits SPL in vivo (Supplementary Fig. 1B–D).^{7, 18} DOP attenuates vascular and immune defects in mouse sepsis¹⁹ and protects against collagen-induced arthritis and experimental autoimmune encephalomyelitis.^{20–22} Yet, little is known regarding its effects on intestinal homeostasis or during IBD. Indeed, intestine-specific deletion of the enzyme actually hastens acute DSS-induced colitis through a yet unknown mechanism.²³

We examined the potential anti-inflammatory effects of SPL inhibition on a TNF-driven model of chronic ileitis (TNFΔARE) that recapitulates many features of Crohn's disease.^{24, 25} First, we analyzed the expression of SPL on lymphocytes via quantitative reverse transcription polymerase chain reaction (Q-PCR) and immunohistochemistry. Next, we investigated the effect of in vivo SPL inhibition on peripheral and tissue immune cell subsets, on the SIP gradient, and on the severity of ileitis. Finally, we examined the underlying mechanism of action of SPL inhibition on intestinal inflammation by studying its effects on the migration of T cells to the terminal ileum, on the induction of leukocyte apoptosis, and on thymocyte maturation.

METHODS

Mice

The B6.129S-Tnf^{f_m2Gkl}/Jarn (TNFΔARE) strain has been previously described.²⁵ TNFΔARE mice were crossed with SIP₁-eGFP^{+/+} reporter mice¹¹ to generate TNFΔARE^{ΔARE/+}/SIP₁-eGFP^{+/+} mice. All mice used for these studies were heterozygous for the ΔARE mutation. They were fed a standard diet

with or without pyridoxine supplementation (Dyets Inc., PA) ad libitum during in vivo studies. Animal procedures were approved by the Institutional Animal Care and Use Committees of the University of California San Diego.

Tissue Fixation, Paraffin Embedding, and Histological Scoring

Tissues were fixed, embedded, cut, and stained with hematoxylin/eosin. The severity of ileitis was assessed in a blinded fashion by a pathologist (P.J.) using a semiquantitative scoring system for murine ileitis, as previously described.²⁶

Cell Isolation

Cells were isolated from the thymus, mesenteric lymph nodes (MLNs), and spleen as previously described.²¹ Lamina propria leukocytes (LPLs) were isolated as described, with slight modification.²⁷ Briefly, ilea were washed with cold phosphate-buffered saline (PBS) and cut into 2-cm pieces, incubated twice with 1X Hank's balanced salt solution (HBSS) containing 1 mM of ethylene diamine tetraacetic acid (EDTA) for 15 minutes at room temperature, followed by digestion with 0.07 mg/mL of Liberase TL and 10 μg/mL of DNase I (Roche Diagnostics, Indianapolis, IN, USA) in RPMI 1640/10% FBS with continuous shaking at 37°C for 60 minutes. The mixture was passed through a 70-μm cell strainer to obtain a single-cell suspension.

Flow Cytometry

Cells from the indicated compartments were suspended in 1X PBS with 2% fetal bovine serum (FBS), supplemented with Fc block and stained with antimouse antibodies against CD4 (RM4-5), CD62L (MEL-14), CD44 (IM7), CD11b (M1/70; Biolegend, San Diego, CA, USA), CD8 (53–6.7), and B220 (RA3-6B2; eBioscience, San Diego, CA, USA) or corresponding isotype controls. Cells were washed twice and fixed in BD stabilizing fixative (BD Biosciences, San Jose, CA, USA). Flow cytometry acquisition was performed using a Cytex DxP10 (Cytex, Fremont, CA, USA). Data were analyzed using FLOWJO software (Tree Star Inc., Ashland, OR, USA).

RNA Extraction, cDNA Synthesis, and Q-PCR

Total RNA was isolated using the RNeasy Kit (Qiagen, Valencia, CA, USA). RNA (500 ng) was reverse-transcribed with a high-capacity cDNA archive kit (Applied Biosystems, Foster City, CA, USA). Q-PCR assays for Sgpl1 (Mm00486079_m1), Tnf (Mm00443258_m1), Il6 (Mm00446190_m1), Il12a (Mm00434169_m1), Ifng (Mm01168134_m1), Il4 (Mm00445259_m1), Il17a (Mm00439618_m1), and Casp3 (Mm01195085_m1) were performed using the TaqMan Universal Master Mix (Applied Biosystems) with Gapdh as endogenous control. Relative gene expression was calculated using the comparative C_T(ΔΔC_T) quantitation method with Applied BioSystems StepOne Software, version 2.3.

Immunohistochemistry

Formalin-fixed, paraffin-embedded sections were deparaffinized and hydrated before antigen retrieval with citrate buffer, pH 6.0, in a prewarmed steamer (NESCO, Two Rivers, WI, USA) for 20 minutes. Sections were incubated for 10 minutes with BLOXALL blocking solution (Vector Laboratories, Burlingame, CA, USA) to quench endogenous peroxidases, followed by incubation with sera to prevent nonspecific antibody binding to Fc-receptors. Pretreatment of tissues with avidin, followed by biotin, was done to block endogenous biotin binding sites (Vector Laboratories). For SPL detection, sections were immunostained with rabbit antimouse SPL polyclonal antibody (Bioss, Woburn, MA, USA) at a 1:200 dilution in PBT (0.5% BSA in PBS with 0.5% Tween-20) at 4°C for overnight. The sections were incubated with biotinylated antirabbit secondary antibody (Vector Laboratories) at 1:1000 in PBT for 30 minutes at room temperature. Sections were incubated with the Elite ABC Kit (Vector Laboratories) for 30 minutes. Signal was detected with DAB (Vector Laboratories) for 2 minutes, and the slides were counterstained with hematoxylin.

SPL Inhibition In Vivo

Mice with established inflammation were treated with DOP (30 mg/L), THI (50 mg/L) (Sigma-Aldrich, St. Louis, MO, USA), or vehicle control for 2 weeks, unless otherwise indicated. Mice were fed a standard diet without pyridoxine supplementation (Dyets Inc., Bethlehem, PA, USA).

S1P Lyase Activity Assay

SPL activity was measured as per published protocol, with some modifications.²⁸ Briefly, tissues were homogenized in tissue protein extraction reagent (T-PER) with protease inhibitors (Halt Protease Inhibitor Cocktail, Thermo Fisher Scientific, Carlsbad, CA, USA), followed by centrifugation at $\times 500g$ for 5 minutes. Ten μL of reaction buffer (0.5 M of potassium phosphate 0.5M, PH 7.5, and 25 μM of sodium orthovanadate) and 10 μL of 125 mM S1P FS (SPL fluorogenic substrate, 1 mg, Cayman Chemical, Ann Arbor, MI, USA) were added to 75 μL of the lysate (25–30 μg) and incubated at 37°C for 6–12 hours. Fluorescence detection was performed at λ_{ex} 325 nm and λ_{em} 420 nm in the presence or absence of 5 mM of semicarbazide (Sigma-Aldrich), a reactive compound that inhibits SPL activity. The activity represents the semicarbazide sensitivity portion of the total activity.

Determination of S1P Levels

S1P was extracted from 200 μL of mouse plasma or tissue homogenate by adding 1 mL of 50/50 dichloromethane/methanol, followed by vortexing for 10 seconds. Samples were spun at 3000 rpm for 5 minutes, and the supernatant was recovered. C¹⁷-S1P was used as an internal standard. The analysis of S1P and sphingosine was carried out using liquid

chromatography–mass spectrometry (LC-MS) as described previously.²⁹

Terminal Deoxynucleotidyl Transferase dUTP Nick End-Labeling Assay

To analyze apoptotic nuclei, 10 μm OCT frozen sections of ileum were prepared and stained according to manufacturer protocol (TACS TdT in situ, Fluorescein, 4812-30-K, R&D systems).

Homing Assays

T cells from spleen and MLNs of TNF Δ ARE mice were sorted using Pan T cell isolation Kit II (Miltenyi Biotec, Auburn, CA, USA) and stained with 3 μM carboxyfluorescein succinimidyl ester (Vybrant CFDA SE Cell Tracer Kit, Thermo Fisher Scientific, Carlsbad, CA, USA) according to the manufacturer's instructions. Twelve million cells were injected intravenously to mice that were pretreated with DOP or vehicle. Twelve to 24 hours later, recipient mice were killed for fluorescently labeled cell quantification of lymphocyte homing.

Cytometry by Time of Flight

Antibody conjugation and staining protocols were obtained from the flow cytometry core at La Jolla Institute for Allergy and Immunology (LJI). Purified antibodies were conjugated with the indicated metals for mass cytometry analysis using the MaxPAR antibody conjugation kit (Fluidigm, San Francisco, CA, USA) according to the manufacturer's instructions. A list of antibodies used for mass cytometry analysis can be found in [Supplementary Table 1](#). Briefly, cells were suspended in 1 mL of cell staining buffer (CSB: 1X CyPBS containing 2 mM of EDTA, 0.1% BSA and 0.05% Na₃N) at 1×10^7 cells mL⁻¹, and cisplatin (DVS Sciences, Cell-ID Cisplatin, 201064) was added at a final concentration of 5 μM for 5 minutes at RT. Cells were stained with antibodies against surface markers for 30 minutes at 4°C and fixed with 2% paraformaldehyde for overnight. Cells were permeabilized and stained with antibodies against intracellular (nuclear proteins) markers and 125-nM DNA intercalator for 30 minutes at room temperature; 1:10th of EQ beads (EQ Four Element Calibration Beads, 201078, Fluidigm) were added to samples, and data were acquired on cytometry by time of flight (CyTOF) Helios mass cytometer (LJI). Computational analyses of mass cytometry data were done with the PhenoGraph algorithm in cytofkit,³⁰ using R studio, version 1.0.153 (<http://www.r-project.org/>), and the cytofkit package, release 3.6, downloaded from Bioconductor (<https://www.bioconductor.org/packages/release/bioc/html/cytofkit.html>), opened in R. Normalized and manually gated singlet (¹⁹¹Iridium (Ir) + ¹⁹³Ir +) viable (¹⁹⁵Platinum (Pt) +) events or singlet (¹⁹¹Ir + ¹⁹³Ir +) viable (¹⁹⁵Pt +) CD3+ MHCII- events were imported into cytofkit, subjected to PhenoGraph analysis, and clustered based on all antibodies (for singlet viable events),

or on all markers excluding parameters gated on for CD3+ MHCII- events (for singlet viable CD3+ MHCII- events), using the following settings: merge method: “ceil” (60,000 events total for live singlet events) or “all” for CD3+ MHCII- events; transformation: cytofAsinh; cluster method: Rphenograph; visualization method: tSNE; and cellular progression: NULL. Results were visualized via the R package “Shiny,” where labels, dot size, and cluster color were customized. Clusters were colored according to phenotype based on the median expression of various markers. The frequency of each cluster and cellular phenotype was determined via .csv files generated by the algorithm. All statistical tests were performed and graphs were generated using GraphPad Prism 7.

Statistical Analysis

Results are expressed as mean \pm SEM unless otherwise indicated. Data were analyzed using GraphPad Prism 7 (GraphPad Software, Inc., San Diego, CA USA). Significant differences between individual groups were calculated using the 2-tailed unpaired *t* test.

RESULTS

S1P Lyase is Highly Expressed in Small Intestine

To investigate the tissue and cellular distribution of SPL, we assessed mRNA transcripts in indicated tissues (Fig. 1A). We noticed that within the gastrointestinal tract, SPL expression was highest in the small bowel, the primary site of inflammation in TNF Δ ARE mice. SPL mRNA expression was assessed in whole ileal tissue and from fractionated epithelial and LPL fractions. SPL expression was highest on the leukocyte fraction, followed by the epithelial fraction (Fig. 1B). Plasma S1P levels were higher than tissue levels (ileum, MLNs, and thymus) (Fig. 1C). Immunohistochemistry localized the expression of SPL to the thymus, MLNs, spleen, and ileum (Fig. 1D). The negative control lacked the primary anti-SPL antibody. Within the thymus, there was higher expression in the medulla compared with the cortex. Within MLNs, SPL expression localized to the deep cortical T-cell zone, whereas in the spleen, SPL was expressed on white pulp nodules, along with red pulp matrix. Interestingly, in the inflamed intestine, SPL signal localized prominently to the epithelium, intraepithelial region, and intestinal crypts, consistent with previous observations.^{23, 31}

S1P Lyase Inhibition Increased Local Tissue S1P Levels, Induced Peripheral Lymphopenia, Downregulated Proinflammatory Cytokines, and Ameliorated Ileitis in TNF Δ ARE Mice

Mice were administered the SPL inhibitor DOP, which competes with pyridoxal 5'-phosphate (PLP) coenzyme, along with a vitamin B6 (pyridoxine)-deficient diet for 2 weeks. After

treatment, the S1P gradient had been obliterated and S1P levels in the ileum, MLNs, and thymus were similar to plasma levels ($*P < 0.05$; $*P < 0.05$; $***P < 0.001$) (Fig. 2A) in treated mice compared with controls. DOP additionally induced peripheral lymphopenia, with a lower frequency and number of blood CD4+ and CD8+ T cells ($***P < 0.001$) compared with controls. By contrast, the frequency and number of B220+ cells were unaffected (Fig. 2B). DOP additionally reduced the ileal mRNA transcripts of TNF, IL-6 ($**P < 0.01$), IL-12 ($*P < 0.05$), IFN- γ , and IL-17 ($**P < 0.01$) compared with controls (Fig. 2C). DOP also attenuated active (granulocytic) inflammation (6.9 ± 1 vs 2.3 ± 2), chronic (lymphocytic/monocytic) inflammation (6.9 ± 1.3 vs 3 ± 1.8), villus distortion (6.6 ± 1.3 vs 3.5 ± 1.4), and the total inflammatory indices (sum of individual indices: 20.5 ± 3.1 vs 8.8 ± 4.7 ; $***P < 0.001$) compared with controls (Fig. 2D). In addition, histological hallmarks of ileitis, such as leukocyte infiltration and hypertrophy of the muscularis propria, were noticeably different (Fig. 2E). DOP significantly inhibited SPL activity ($*P < 0.05$) in the ileum without affecting SPL mRNA transcripts (Supplementary Fig. 1C, D). A pyridoxine-deficient diet alone did not induce lymphopenia or affect the severity of ileitis, compared with a standard diet (Supplementary Fig. 2A–C). In DOP-treated mice, the lymphopenic effect was greater on circulating naïve CD4+ and CD8+ T cells ($***P < 0.001$); thereby, the percentage of effector T cells increased ($***P < 0.001$) in the DOP-treated group compared with controls (Supplementary Fig. 3A, B). In addition, the median fluorescence intensity (MFI) of S1PR1 on CD4+, CD8+ T ($**P < 0.01$), and B220+ ($*P < 0.05$) cells was lower in the DOP-treated group compared with controls (Supplementary Fig. 3C, D). We observed a lymphopenic effect on circulating T cells as early as 24 hours after DOP treatment (data not shown). However, although DOP treatment for 1 week significantly reduced circulating T cells, it did not affect ileitis severity (Supplementary Fig. 4A–C). Taken together, these results demonstrate that SPL inhibition abolishes the S1P gradient, potentially altering cell recruitment and/or egress to/from the intestine. SPL inhibition predominantly decreased naïve CD4+ T-cell and CD8+ T-cell subsets from circulation, downregulated S1PR1 surface expression on lymphocytes, decreased proinflammatory cytokine transcripts in the intestine, and attenuated chronic ileitis.

DOP Prominently Depletes Naïve CD4 and CD8+ T-Cell Subsets Within Immune Compartments

We then assessed the effects of DOP treatment for 2 weeks on lymphocytes and monocytes within relevant immune compartments (ie, spleen, MLNs, and ileal LP). Total cell counts were uniformly reduced in the spleen ($****P < 0.0001$), MLNs ($**P < 0.01$), and ileal LP ($*P < 0.05$) after DOP, compared with controls (Fig. 3A–C). However, SPL inhibition differentially affected lymphocyte subsets with reduced

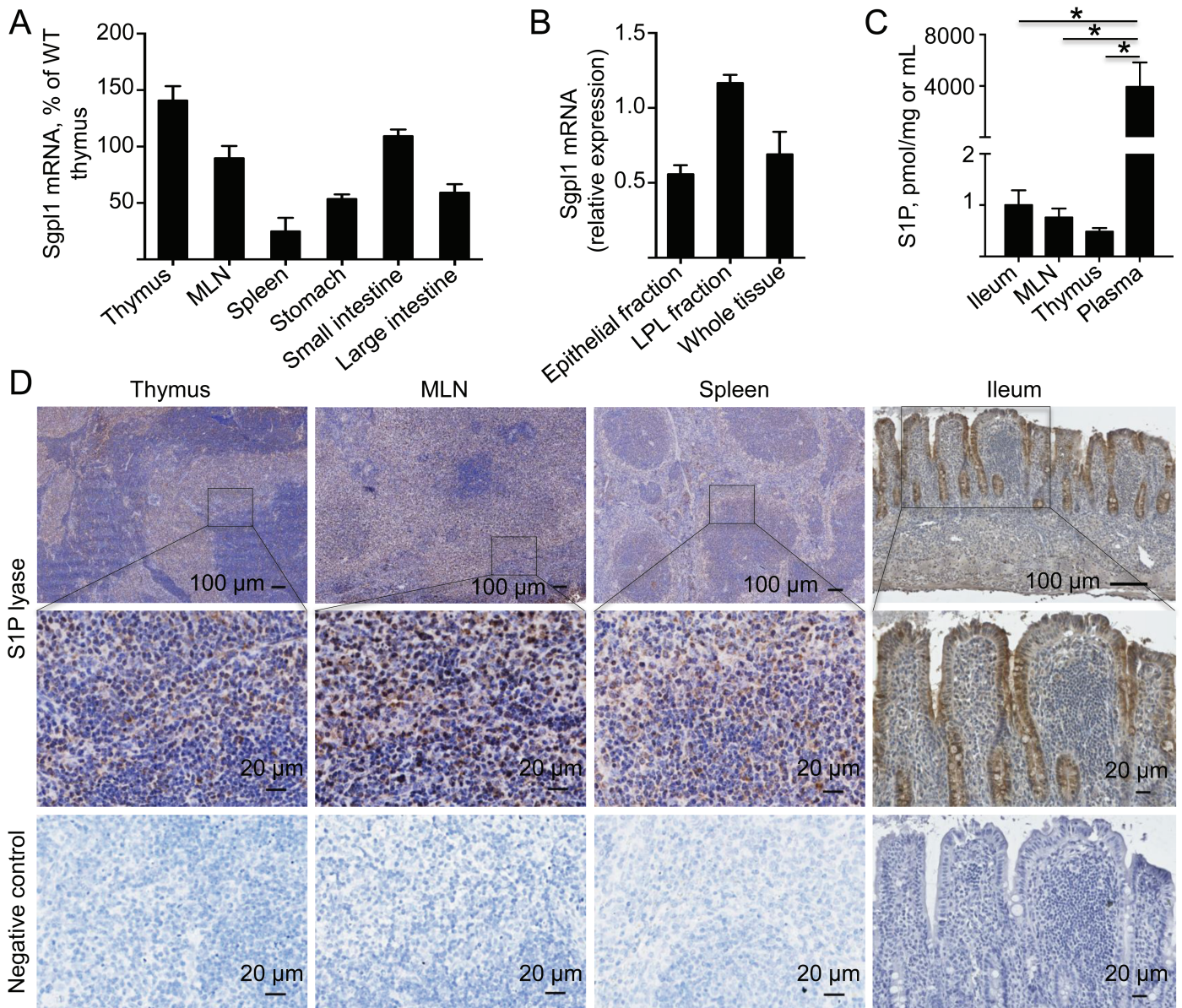


FIGURE 1. Tissue and cellular distribution of S1P lyase in mice with chronic ileitis. A, SPL mRNA transcripts (Sgpl1) were assessed by real-time RTPCR in indicated tissues of 10-week-old TNFΔARE mice with established ileitis. B, SPL mRNA expression in epithelial cells, lamina propria leukocyte (LPL) fractions, and whole ileal tissue relative to GAPDH. C, Tissue and plasma S1P levels were measured using the LC-MS platform. D, Localization of the SPL protein in indicated tissues was assessed by immunohistochemistry (representative images). Data are expressed as mean ± SEM, n ≥ 4 mice/group (*P < 0.05).

CD4+ and CD8+ T cells (****P < 0.0001), but without an effect on B cells in any of these 3 compartments (Fig. 3A–C). In the ileal lamina propria, we observed a modest decrease in the frequency of CD8+ T cells (**P < 0.01) and myeloid cells (CD11b+; *P < 0.05) (Fig. 3C). Further subset analyses identified the most noticeable effects on splenic naïve CD4+ and CD8+ T cells after DOP treatment (Fig. 3A–C), yet the total cell counts were markedly decreased in all compartments assessed.

Deep Immunophenotyping of Leukocyte Subsets After S1P Lyase Inhibition in TNFΔARE Mice

We next investigated the breadth of the effect of DOP on leukocyte subsets via high-dimension mass cytometry (CyTOF) analysis on a small number of DOP and vehicle-treated mice (n = 3/treatment). Cells from blood, MLNs, and ileal LP were stained with a panel of 34 metal-conjugated

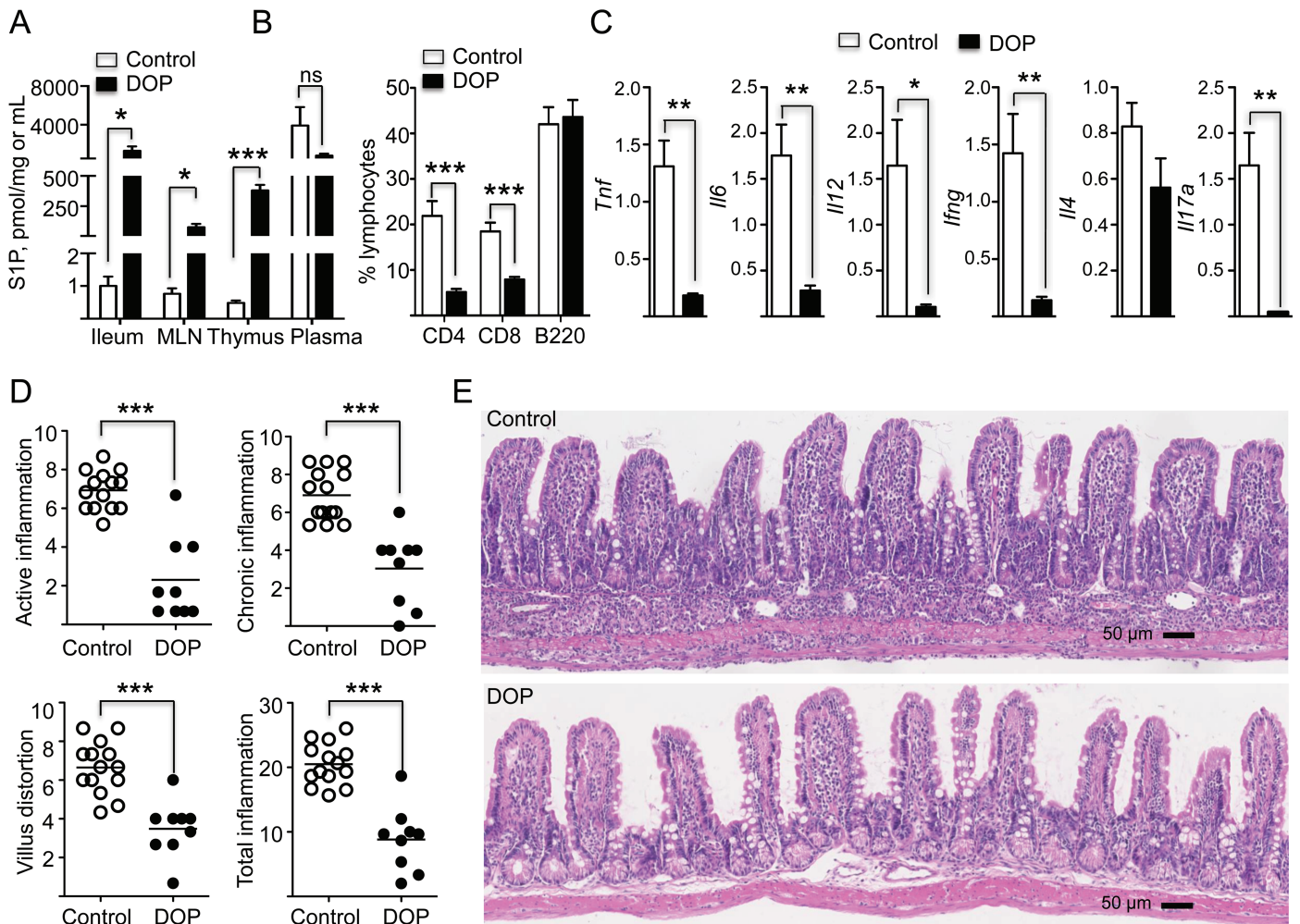


FIGURE 2. S1P lyase inhibition increased tissue S1P levels, obliterated its gradient, induced lymphopenia, downregulated proinflammatory cytokines in the intestine, and ameliorated chronic ileitis. **A**, Tissue and plasma S1P levels in TNF Δ ARE mice treated with DOP or vehicle were measured using the LC-MS platform. **B**, Percentage of indicated lymphocyte subsets in the peripheral blood of TNF Δ ARE mice treated with DOP or vehicle for 2 weeks. **C**, mRNA transcripts of indicated proinflammatory cytokines relative to GAPDH in the ileum of 12-week-old TNF Δ ARE mice treated with DOP or vehicle control. **D**, Semiquantitative histopathological assessment of the effects of DOP treatment and vehicle on the severity of ileitis in TNF Δ ARE mice: active inflammation, chronic inflammation, villus distortion, and total inflammatory indices, respectively, as read by a gastrointestinal pathologist in a blinded fashion. Data are expressed as mean \pm SEM; $n \geq 9$ mice/group (*** $P < 0.001$; ** $P < 0.01$; * $P < 0.05$ by 2-tailed t test). **E**, Representative micrographs of the effects of DOP on intestinal architecture and inflammatory infiltrate (hematoxylin and eosin, 10 \times magnification).

antibodies (Supplementary Table 1), acquired using a Helios 2 mass cytometer and analyzed using the PhenoGraph algorithm. In peripheral blood, DOP treatment resulted in a pronounced decrease in both CD4⁺ and CD8⁺ T cells, consistent with findings observed via flow in the spleen, with an intermediate decrease in the frequency of CD19⁺ B cells and a significantly increased frequency of CD11b⁺ myeloid cells (Supplemental Fig. 5A, B), different from what was observed in the spleen via flow cytometry. Cytof similarly showed that DOP treatment decreased naïve CD4⁺ and CD8⁺ T cells, with a trend toward increased frequency of CD44^{high} effector CD4⁺ and CD8⁺ T cells (Supplemental Fig. 5C–E). In contrast, compared with peripheral blood, the distribution of leukocyte

subsets showed only minimal alterations in MLNs and ileal LP after DOP treatment, despite the major effects on the cell counts observed by flow cytometry in the MLNs and ileum (Fig. 3A–C). In the MLNs, there was no overall change in the relative frequencies of CD4⁺ and CD8⁺ T cells, CD11b⁺ myeloid cells, or CD19⁺ B cells, with a modest decrease in central memory CD4⁺ T cells and a modest increase in the frequency of CD44^{high} effector CD8⁺ T cells (Supplemental Fig. 5F–J). Similarly, in ileal LP, DOP treatment was associated with a modest decrease in the frequency of CD8⁺ T cells and trends toward decreased frequency of CD11b⁺ myeloid cells and of CD19⁺ B cells. Ileal LP T-cell subsets showed no statistically significant changes in the cell percentages after DOP treatment

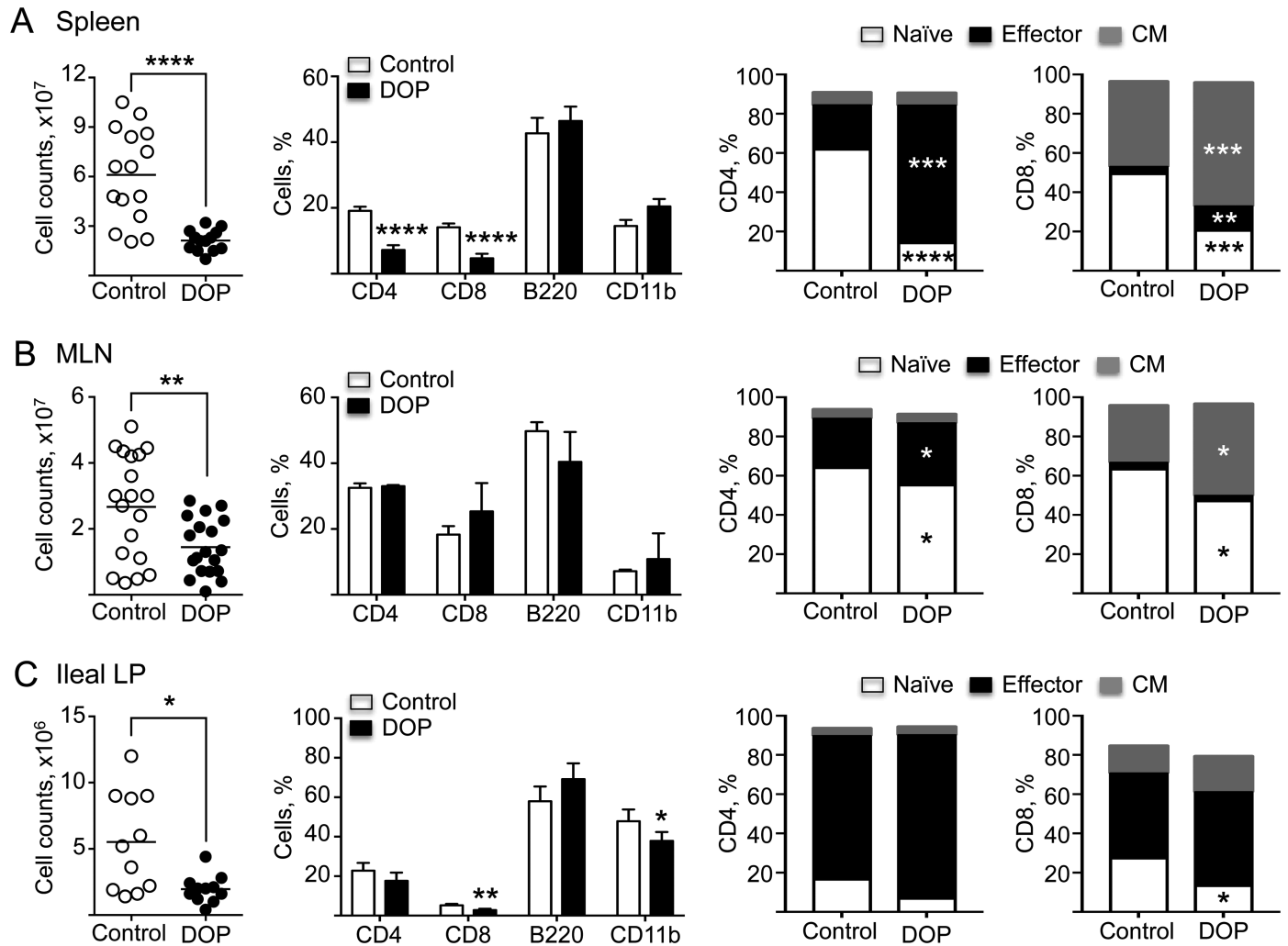


FIGURE 3. Effects of DOP on cell subsets within immune compartments. Cell counts and subset flow cytometry analyses of (A) spleen, (B) MLNs, and (C) ileal LP of TNFΔARE mice treated with DOP or vehicle control for 2 weeks. Data are from 3 independent experiments, expressed as mean ± SEM; n ≥ 10 mice/group (**P* < 0.05; ***P* < 0.01; ****P* < 0.001; *****P* < 0.0001 by 2-tailed *t* test).

(Supplemental Fig. 5K–O). These high-dimensional data corroborate overall trends observed with the flow cytometry-based studies (major percentage shifts observed in blood/spleen) but not in the MLNs and ileum, where DOP similarly decreases all leukocyte types, without singularly affecting specific cell subsets.

The Lymphopenic Effect of 2-acetyl-4 (tetrahydroxybutyl)imidazole Is Independent of its Anti-inflammatory Activity

The safety of the SPL inhibitor THI has been tested in patients with rheumatoid arthritis.^{18, 20} To assess its potential anti-inflammatory effects on ileitis, 10-week-old TNFΔARE mice were administered THI in drinking water for 2 and 4 weeks. THI induced peripheral lymphopenia of CD4+ T cells

(***P* < 0.01) and CD8+ T cells (***P* < 0.001), but like DOP, it had no significant effect on peripheral B220+ cells compared with vehicle-treated controls (Fig. 4A). Also, different from DOP, histopathological analysis did not show an anti-inflammatory effect in mice treated for 2 or 4 weeks (Fig. 4B). To further understand the lack of a therapeutic effect of THI, we assessed S1P levels and found no significant changes in the ileum, MLNs, or plasma S1P in THI-treated mice compared with controls (Fig. 4C). Similarly, THI had no effect on overall S1PR1 expression (MFI) on CD4/8 or B220+ lymphocytes (Fig. 4D, E). These results suggest that the lymphopenic effect of THI is independent of its anti-inflammatory activity on ileitis and that the mechanism of action of these drugs is not solely predicated on its ability to induce peripheral lymphopenia.

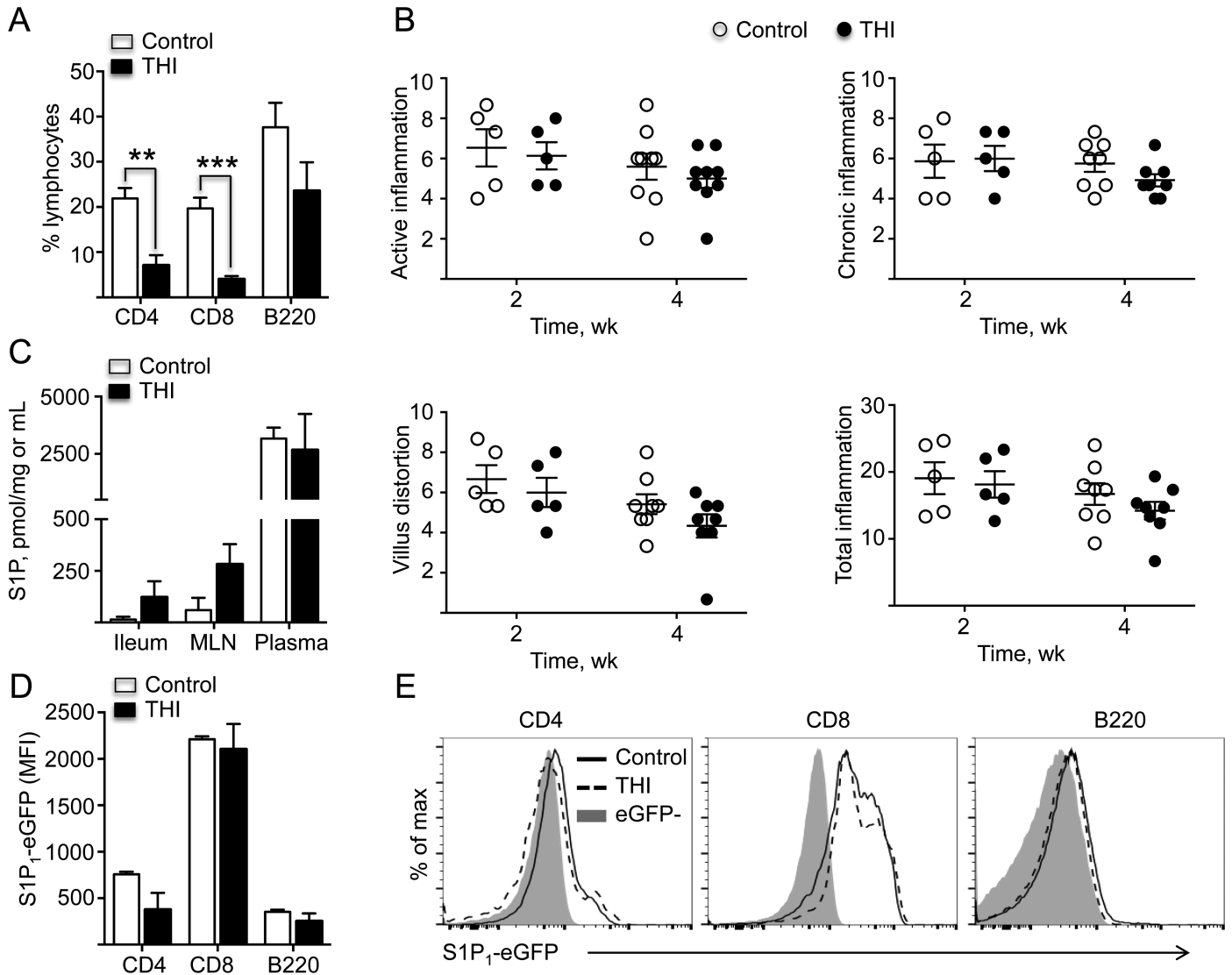


FIGURE 4. THI treatment induced peripheral lymphopenia but did not ameliorate ileitis. A, Percentage of indicated lymphocytes in peripheral blood of TNFΔARE mice treated with THI or vehicle control. B, Histopathological analyses of TNFΔARE ileum from mice treated with THI or vehicle. Graphs indicate active (neutrophilic) inflammation, chronic (lymphocyte, monocytes) inflammation, villus distortion, and the total inflammatory indexes, respectively, as previously described.²⁶ C, Tissue and plasma S1P levels in TNFΔARE mice treated with THI or vehicle, as measured using LC-MS platforms. D, E, Bar graph and histograms represent S1P₁ expression (median fluorescence intensity) of indicated cell subsets from blood of TNFΔARE mice treated with THI or vehicle control. Data are expressed as mean ± SEM; n ≥ 5 mice/group (**P < 0.01, ***P < 0.001 by 2-tailed t test).

S1P Lyase Inhibition Did Not Alter the Short-term Homing of T Cells to the Intestine

Given the known effects of S1P on tightening the lymphatic endothelial barrier, we hypothesized that elevated local S1P levels could similarly enhance the endothelial barrier at postcapillary venules and impede leukocyte transmigration and recruitment to the intestine.^{13, 32-35} To test this hypothesis, we isolated and labeled negatively-selected T cells with CFSE (after depleting B cells) and injected them into 10-week-old TNFΔARE mice that had received DOP or vehicle for 48 hours before transfer. Cells were

allowed to traffic for 24 hours to quantify the number of cells able to home to different compartments via flow cytometry. Analysis showed a significant (**P < 0.01) accumulation of CFSE+ cells in the spleen of recipient mice treated with DOP compared with vehicle controls, but no effect on traffic to the thymus, MLNs, or ileal LP (Fig. 5). Subset analysis revealed a preponderance of naïve CD4+ T cells retained in the spleen (Fig. 5). Thus, the anti-inflammatory effect of DOP is not mediated by interference with de novo recruitment of T cells to the intestine, as has been argued for anti-integrin therapies.

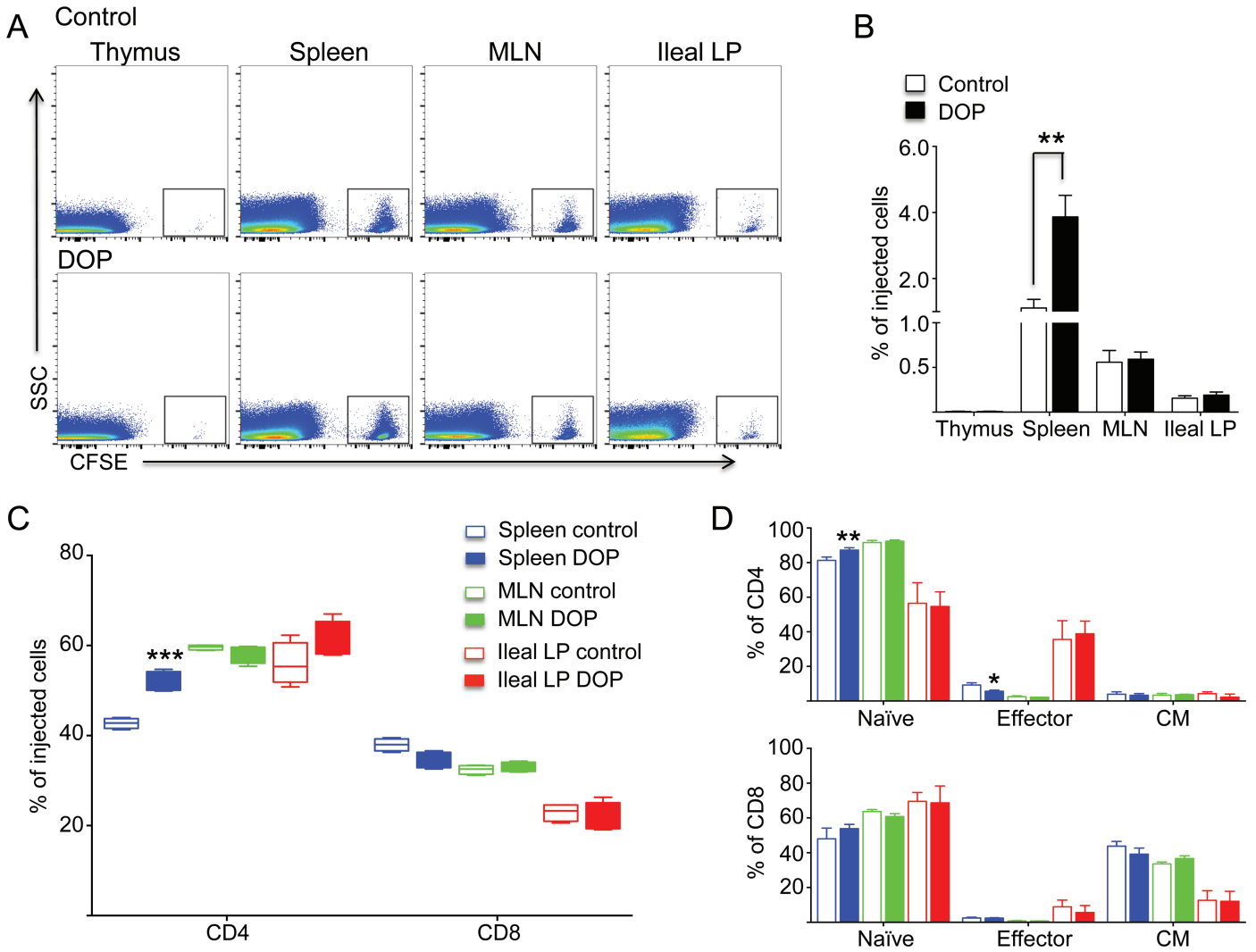


FIGURE 5. S1P lyase inhibition did not alter de novo T-cell recruitment to the intestine. A, B, Effect of DOP on the frequency of total CFSE-labeled T cells migrating to the thymus, spleen, MLNs, and ileal LP of recipient TNFΔARE mice. C, Effect of DOP on the frequency of CFSE-labeled CD4+ and CD8+ T cells migrating to the spleen, MLNs, and ileal LP. D, Analyses of naïve, effector, and central memory subsets within the CD4 and CD8+ T cells migrating to indicated sites. Data are from 3 independent experiments expressed as mean ± SEM; n ≥ 10 mice/group (*P < 0.05, **P < 0.01, ***P < 0.001 by 2-tailed t test).

S1P Lyase Inhibition Did Not Induce Apoptosis of Infiltrating Leukocytes in TNFΔARE Mice

Elevated S1P levels result in accumulation of ceramide, a lipid upstream of S1P, which is known to induce T-cell apoptosis.³⁶ We hypothesized that elevated S1P levels should increase all upstream metabolites, leading to increased local ceramide levels and leukocyte apoptosis in the intestine. However, we did not observe changes in the percentage of apoptotic CD4, CD8, or total cells via annexin V staining in cells from the ileal LP of mice treated with DOP for 2 days, 1 week, or 2 weeks (Fig. 6A). Caspase 3 levels were unchanged despite a dramatic increase in sphingosine upstream of S1P (Fig. 6B, C). Similarly, terminal deoxynucleotidyl transferase dUTP nick end-labeling (TUNEL) analysis did not show significant changes in the

number of apoptotic nucleated cells in the ileal crypts or villi of DOP-treated mice compared with controls (Fig. 6D). These results suggest that the anti-inflammatory effects of SPL inhibition are not mediated by the induction of leukocyte apoptosis by ceramide in the chronically inflamed intestine of TNFΔARE mice.

S1P Lyase Inhibition Promoted Thymic Involution and Cortical Atrophy by Depletion of Stage II CD4+/CD8+ (Double-Positive) T Cells in TNFΔARE Mice

Finally, we examined whether the anti-inflammatory effect could be due to central immunosuppression.³⁷ Thymic

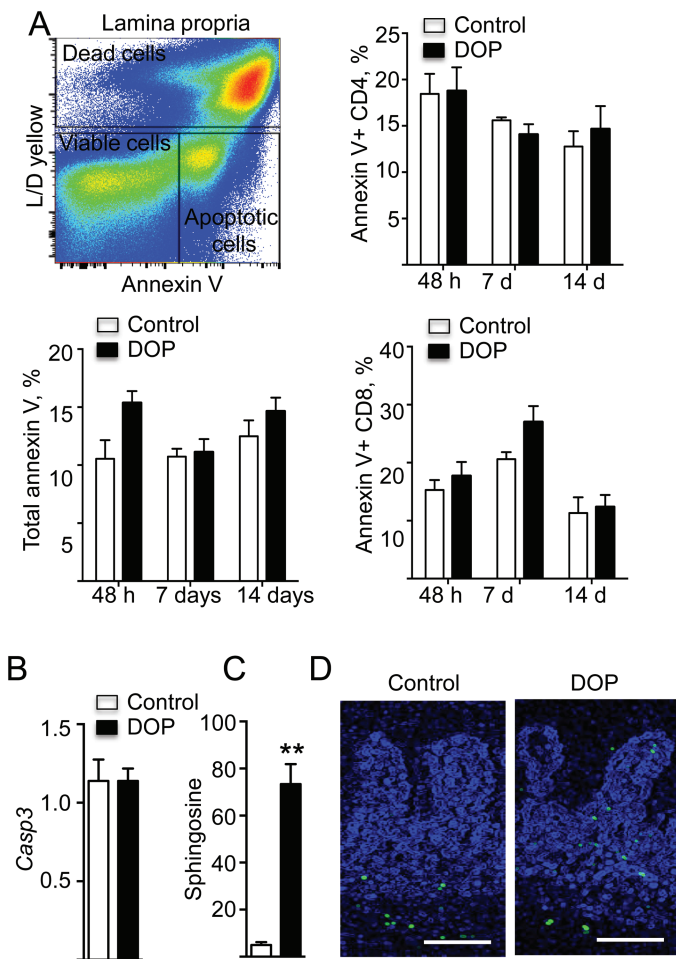


FIGURE 6. S1P lyase inhibition did not induce leukocyte apoptosis in the intestine in mice with chronic ileitis. **A**, Annexin V staining total CD4+ and CD8+ T cells isolated from TNFΔARE mice treated with DOP or vehicle (control) for the indicated number of days. Data are expressed as mean ± SEM; n ≥ 4 mice/group/time point. **B**, Caspase 3 mRNA transcripts relative to GAPDH as quantified by real time Q-PCR after 2 weeks of DOP treatment. Data are expressed as mean ± SEM, n ≥ 9 mice/group. **C**, Sphingosine levels in the ileum of DOP- and vehicle-treated mice. Data are expressed as mean ± SEM; n ≥ 9 mice/group (***P* < 0.01 by 2-tailed *t* test). **D**, TUNEL staining of the ileum of TNFΔARE mice treated for 2 weeks with DOP and vehicle control. Representative images are from 3 independent experiments. Scale bar = 100 μm.

size, weight, and cell counts (***P* < 0.001) were markedly reduced in DOP-treated mice compared with controls (Fig. 7A). Reduction in thymic size was progressive with DOP administration over 2, 4, 6, 8, 10, and 14 days (Supplementary Fig. 6). In the DOP-treated group, the cortical region showed atrophy over time (data not shown), with marked atrophy by day 14, as evidenced by near absence of corticomedullary demarcation (Fig. 7B, C). The percentage of CD4+C8+ double-positive thymocytes in the DOP group progressively decreased, compared with controls (1% ± 1% vs 69% ± 16% at day 14). This decrease in

CD4+CD8+ double-positive thymocytes occurred in parallel with a relative increase in CD4+CD8- and CD4-CD8+ single-positive thymocytes over time. On day 14, most of the cells left in the thymus were CD4+CD8- (55% ± 5% vs 15% ± 6%) and CD4-CD8+ (37% ± 3% vs 7% ± 4%) single-positive cells, compared with controls (Fig. 7D). These results suggest that thymic involution and interference with T-cell maturation play a major role on the anti-inflammatory effect of SPL inhibition.³⁷

DISCUSSION

Drugs that target the S1P axis are rapidly advancing through the IBD clinical trial pipeline.³⁸ Fingolimod has been approved for the treatment of multiple sclerosis, ozanimod is currently on phase 3 trials both for UC and CD, and etrasimod has recently completed phase 2 in UC.³⁹

In previous studies, we observed that the S1P-degrading enzymes (S1P phosphatases and SPL) were downregulated in the ilea of IBD mouse models and in patients with IBD,⁴⁰ which could potentially represent a retention signal that impedes the recirculation of lymphocytes, contributing to their accumulation in inflamed tissues over time.^{41, 42} Studies by Schwab and Cyster⁷ showed that lymphocyte egress from lymphoid tissue is mediated by S1P gradients through the activity of SPL. SPL inhibition increased S1P levels in lymphoid tissues such as the thymus, spleen, and lymph nodes and downregulated S1PR1 expression on lymphocytes. However, the role of SPL during intestinal homeostasis and chronic intestinal inflammation had not been examined. Indeed, in a prior study, acute DSS colitis was aggravated by SPL inhibition.²³ In the present study, we show that SPL is ubiquitously expressed; however, within the intestine, SPL is predominantly localized to the epithelium and infiltrating leukocytes, predominantly of the small intestine. As the small intestine is the main intestinal segment affected in TNFΔARE mice, this model of IBD might be of particular translational relevance. Here, we demonstrate that local S1P levels can be manipulated for therapeutic purposes during experimental IBD. S1P levels are high in plasma and low in the ileum, MLNs, and thymus of uninflamed controls and inflamed TNFΔARE mice. S1P levels were higher in the plasma of inflamed mice, compared with those of uninflamed mice, which may partially explain increased recirculation of immune cells from the inflamed intestine. We further demonstrate that although SPL inhibition did not alter S1P levels in plasma, it markedly increased S1P tissue levels from about 1 picomol/mg to 100, 400, and 2000 picomol/mg in the MLNs, thymus, and ileum of TNFΔARE mice, respectively. SPL inhibition induced peripheral lymphopenia and downregulated S1PR1 expression (desensitization) on circulating lymphocytes, as shown previously in healthy mice.⁷ Yet in the present study, we show a major therapeutic effect on ileitis, with a marked decrease of inflammatory cells in the spleen, MLNs, and ileum. There was additionally reversal of villus atrophy and crypt and muscularis hypertrophy along with downregulation of proinflammatory

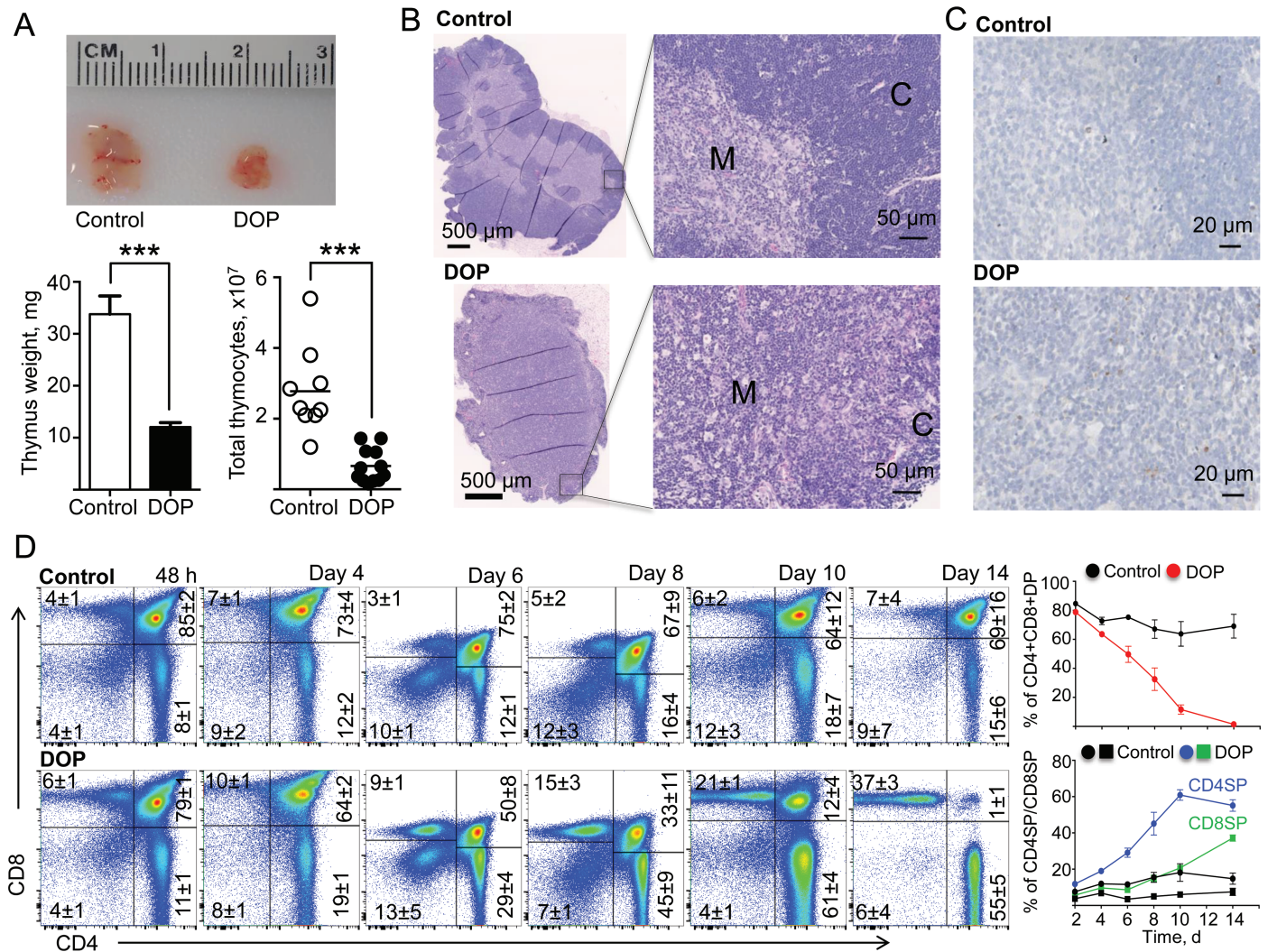


FIGURE 7. S1P lyase inhibition promoted atrophy of the thymic cortex and depletion of stage II (double-positive CD4/CD8) T cells in TNFΔARE mice. A, Representative images, weights (mg), and total number of thymocytes from TNFΔARE mice treated with DOP or vehicle control for 2 weeks. B, Representative hematoxylin and eosin–stained sections and (C) cleaved-caspase-3 staining of the thymus of DOP- and vehicle-treated TNFΔARE mice for 2 weeks (C, cortex; M, medulla). D, Representative dot plots and CD4/CD8 percentages of thymocytes from TNFΔARE mice treated with DOP or vehicle for 2 weeks or indicated times. Data are expressed as mean \pm SEM; $n \geq 5$ mice/group/time point (** $P < 0.001$ by 2-tailed t test). Abbreviations: DP, double-positive (CD4+/CD8+) cells; SP, single-positive mature CD4+CD8- or CD4-CD8+ cells.

cytokine transcripts (ie, TNF, IL-6, IL-12, IFN- γ , and IL-17) in the ileum of mice with chronic ileitis. Although the SPL inhibitor THI^{7, 18, 31} induced significant lymphopenia, it did not ameliorate ileitis after 2- or 4-week administration, suggesting that the anti-inflammatory effects of these compounds might be independent of their ability to deplete peripheral T cells.

During IBD, there is dysregulated recruitment of leukocytes in response to elevated chemoattractants and enhanced expression of integrin ligands (eg, MAdCAM-1, VCAM-1), which contribute to the pathogenesis of the disease.^{43, 44} The proposed mechanism of action of antibodies against integrins $\alpha 4\beta 1/\alpha 4\beta 7$ (ie, natalizumab), $\alpha 4\beta 7$ (ie, vedolizumab), and $\beta 7$ (ie, etrolizumab) is interference with the binding of integrins on

the lymphocyte surface with their respective endothelial ligands (ie, VCAM-1, MAdCAM-1) at postcapillary venules. By contrast, S1P receptor modulators are believed to act by blocking lymphocyte egress from secondary lymphoid organs. Although we considered that SPL inhibitors may exert their anti-inflammatory activity by tightening the endothelial barrier and decreasing recruitment at postcapillary venules, we found that SPL inhibition did not affect de novo recruitment of CD4+ T cells to the MLNs or intestine.⁴⁵ Yet DOP markedly decreased the overall inflammatory infiltrate in all relevant sites (LP, MLNs, and spleen).⁴⁶ However, we found a profound reshaping of the lymphocyte-to-myeloid ratio in peripheral blood after DOP treatment. The high-dimensional approach emphasized

the compartment-specific effects of SPL inhibition on leukocyte distribution (predominantly observed in peripheral blood, followed by spleen), whereas in the MLNs and ileum we observed an overall depletion of cell counts of most cell types, without major effects on specific cellular subsets.

Many immunosuppressive drugs in current clinical use are believed to work in part by inducing apoptosis of inflammatory cells within the lamina propria.⁴⁷ Ceramide, a known proapoptotic molecule, may potentially mediate this effect after SPL inhibition.³⁶ Although we did not directly measure ceramide, there was marked elevation of sphingosine levels in DOP-treated mice. As ceramide is 1 step upstream of sphingosine, our findings suggest that ceramide levels may be similarly increased.⁴⁸ However, there were no significant changes in the number of apoptotic cells in the ileum of TNF Δ ARE mice at any time point (early or late), either by annexin V staining or by TUNEL assay. Thus, it is unlikely that the anti-inflammatory properties are mediated by induction of leukocyte apoptosis within the intestinal lamina propria.

By contrast, in the thymus DOP had a remarkable effect on thymic mass and cell counts, similar to what has been reported after long-term administration of S1PR agonist fingolimod in rodents.^{47, 49} DOP treatment induced marked thymus involution, with disappearance of the cortical region and near absence of immature CD4+C8+ double-positive thymocytes, along with a relative increase in mature CD4+CD8- and CD4-CD8+ single-positive thymocytes. SPL was expressed predominantly in the medulla. Its action of degrading S1P allows for S1PR1 re-expression (resensitization) and egress on mature thymocytes by maintaining low thymic S1P levels.⁵⁰ However, lyase inhibitors induced mature thymocytes to accumulate in the thymic medulla, where they may eventually undergo apoptosis. Our findings support the hypothesis that the anti-inflammatory effects of SPL inhibition on chronic ileitis are mediated by central immune suppression and interference with thymocyte maturation.

In summary, our studies demonstrate the remarkable anti-inflammatory activity of SPL inhibition in a chronic model of Crohn's-like ileitis after obliteration of the S1P gradient. SPL inhibition downregulated proinflammatory cytokines, reduced inflammatory infiltrates, and restored intestinal architecture. Based on our findings, we hypothesize that short-term treatment with these agents may modulate overactive T-cell immune responses, as seen in IBD and other T-cell-mediated diseases. Whether this strategy might be too immunosuppressive in humans and result in serious opportunistic infections will likely depend on the timing of recovery and restoration of lymphocyte counts after discontinuation of therapy.

SUPPLEMENTARY DATA

Supplementary data are available at *Inflammatory Bowel Diseases* online.

ACKNOWLEDGEMENTS

We thank Lauren Gima and Joshua Delos Boyer for technical assistance.

REFERENCES

- Rivera-Nieves J. Targeting leukocyte traffic: a new era for the treatment of inflammatory bowel disease. *J Crohns Colitis*. 2018;12:S631–S632.
- Ghosh S, Goldin E, Gordon FH, et al; Natalizumab Pan-European Study Group. Natalizumab for active Crohn's disease. *N Engl J Med*. 2003;348:24–32.
- Feagan BG, Rutgeerts P, Sands BE, et al; GEMINI 1 Study Group. Vedolizumab as induction and maintenance therapy for ulcerative colitis. *N Engl J Med*. 2013;369:699–710.
- Major EO. Progressive multifocal leukoencephalopathy in patients on immunomodulatory therapies. *Annu Rev Med*. 2010;61:35–47.
- Cyster JG. Chemokines, sphingosine-1-phosphate, and cell migration in secondary lymphoid organs. *Annu Rev Immunol*. 2005;23:127–159.
- Matloubian M, Lo CG, Cinamon G, et al. Lymphocyte egress from thymus and peripheral lymphoid organs is dependent on SIP receptor 1. *Nature*. 2004;427:355–360.
- Schwab SR, Pereira JP, Matloubian M, et al. Lymphocyte sequestration through S1P lyase inhibition and disruption of S1P gradients. *Science*. 2005;309:1735–1739.
- Rivera J, Proia RL, Olivera A. The alliance of sphingosine-1-phosphate and its receptors in immunity. *Nat Rev Immunol*. 2008;8:753–763.
- Sandborn WJ, Feagan BG, Wolf DC, et al; TOUCHSTONE Study Group. Ozanimod induction and maintenance treatment for ulcerative colitis. *N Engl J Med*. 2016;374:1754–1762.
- Marchese A, Benovic JL. Ubiquitination of G-protein-coupled receptors. *Methods Mol Biol*. 2004;259:299–305.
- Cahalan SM, Gonzalez-Cabrera PJ, Sarkisyan G, et al. Actions of a picomolar short-acting S1P₁ agonist in S1P₁-eGFP knock-in mice. *Nat Chem Biol*. 2011;7:254–256.
- Serra M, Saba JD. Sphingosine 1-phosphate lyase, a key regulator of sphingosine 1-phosphate signaling and function. *Adv Enzyme Regul*. 2010;50:349–362.
- Montrose DC, Scherl EJ, Bosworth BP, et al. S1P₁ localizes to the colonic vasculature in ulcerative colitis and maintains blood vessel integrity. *J Lipid Res*. 2013;54:843–851.
- Sanchez T, Estrada-Hernandez T, Paik JH, et al. Phosphorylation and action of the immunomodulator FTY720 inhibits vascular endothelial cell growth factor-induced vascular permeability. *J Biol Chem*. 2003;278:47281–47290.
- Zondag GC, Postma FR, Etten IV, et al. Sphingosine 1-phosphate signalling through the G-protein-coupled receptor Edg-1. *Biochem J*. 1998;330 (Pt 2):605–609.
- Rosen H, Gonzalez-Cabrera PJ, Sanna MG, et al. Sphingosine 1-phosphate receptor signaling. *Annu Rev Biochem*. 2009;78:743–768.
- Sanllehi P, Abad JL, Casas J, et al. Inhibitors of sphingosine-1-phosphate metabolism (sphingosine kinases and sphingosine-1-phosphate lyase). *Chem Phys Lipids*. 2016;197:69–81.
- Bagdanoff JT, Donoviel MS, Nouraldeen A, et al. Inhibition of sphingosine 1-phosphate lyase for the treatment of rheumatoid arthritis: discovery of (E)-1-(4-((1R,2S,3R)-1,2,3,4-tetrahydroxybutyl)-1H-imidazol-2-yl)ethanone oxime (LX2931) and (1R,2S,3R)-1-(2-(isoxazol-3-yl)-1H-imidazol-4-yl)butane-1,2,3,4-tetraol (LX2932). *J Med Chem*. 2010;53:8650–8662.
- Hemdan NY, Weigel C, Reimann CM, et al. Modulating sphingosine 1-phosphate signaling with DOP or FTY720 alleviates vascular and immune defects in mouse sepsis. *Eur J Immunol*. 2016;46:2767–2777.
- Bagdanoff JT, Donoviel MS, Nouraldeen A, et al. Inhibition of sphingosine-1-phosphate lyase for the treatment of autoimmune disorders. *J Med Chem*. 2009;52:3941–3953.
- Billich A, Baumruker T, Beerli C, et al. Partial deficiency of sphingosine-1-phosphate lyase confers protection in experimental autoimmune encephalomyelitis. *PLoS One*. 2013;8:e59630.
- Weiler S, Braendlin N, Beerli C, et al. Orally active 7-substituted (4-benzylphthalazin-1-yl)-2-methylpiperazin-1-yl]nicotinonitriles as active-site inhibitors of sphingosine 1-phosphate lyase for the treatment of multiple sclerosis. *J Med Chem*. 2014;57:5074–5084.
- Degagné E, Pandurangan A, Bandhuvula P, et al. Sphingosine-1-phosphate lyase downregulation promotes colon carcinogenesis through STAT3-activated microRNAs. *J Clin Invest*. 2014;124:5368–5384.
- Ho J, Kurtz CC, Naganuma M, et al. A CD8+/CD103^{HIGH} T cell subset regulates TNF-mediated chronic murine ileitis. *J Immunol*. 2008;180:2573–2580.
- Kontoyannis D, Pasparakis M, Pizarro TT, et al. Impaired on/off regulation of TNF biosynthesis in mice lacking TNF AU-rich elements: implications for joint and gut-associated immunopathologies. *Immunity*. 1999;10:387–398.
- Burns RC, Rivera-Nieves J, Moskaluk CA, et al. Antibody blockade of ICAM-1 and VCAM-1 ameliorates inflammation in the SAMP-1/Yit adoptive transfer model of Crohn's disease in mice. *Gastroenterology*. 2001;121:1428–1436.

27. Bamias G, Martin C, Mishina M, et al. Proinflammatory effects of TH2 cytokines in a murine model of chronic small intestinal inflammation. *Gastroenterology*. 2005;128:654–666.
28. Bedia C, Camacho L, Casas J, et al. Synthesis of a fluorogenic analogue of sphingosine-1-phosphate and its use to determine sphingosine-1-phosphate lyase activity. *Chembiochem*. 2009;10:820–822.
29. Quehenberger O, Armando AM, Brown AH, et al. Lipidomics reveals a remarkable diversity of lipids in human plasma. *J Lipid Res*. 2010;51:3299–3305.
30. Chen H, Lau MC, Wong MT, et al. Cytokit: a bioconductor package for an integrated mass cytometry data analysis pipeline. *PLoS Comput Biol*. 2016;12:e1005112.
31. Ohtoyo M, Machinaga N, Inoue R, et al. Component of caramel food coloring, THI, causes lymphopenia indirectly via a key metabolic intermediate. *Cell Chem Biol*. 2016;23:555–560.
32. Yopp AC, Ochando JC, Mao M, et al. Sphingosine 1-phosphate receptors regulate chemokine-driven transendothelial migration of lymph node but not splenic T cells. *J Immunol*. 2005;175:2913–2924.
33. McVerry BJ, Garcia JG. In vitro and in vivo modulation of vascular barrier integrity by sphingosine 1-phosphate: mechanistic insights. *Cell Signal*. 2005;17:131–139.
34. McVerry BJ, Peng X, Hassoun PM, et al. Sphingosine 1-phosphate reduces vascular leak in murine and canine models of acute lung injury. *Am J Respir Crit Care Med*. 2004;170:987–993.
35. Wei SH, Rosen H, Matheu MP, et al. Sphingosine 1-phosphate type 1 receptor agonism inhibits transendothelial migration of medullary T cells to lymphatic sinuses. *Nat Immunol*. 2005;6:1228–1235.
36. Obeid LM, Hannun YA. Ceramide: a stress signal and mediator of growth suppression and apoptosis. *J Cell Biochem*. 1995;58:191–198.
37. Allende ML, Dreier JL, Mandala S, et al. Expression of the sphingosine 1-phosphate receptor, S1P1, on T-cells controls thymic emigration. *J Biol Chem*. 2004;279:15396–15401.
38. Peyrin-Biroulet L, Christopher R, Behan D, et al. Modulation of sphingosine-1-phosphate in inflammatory bowel disease. *Autoimmun Rev*. 2017;16:495–503.
39. Kunkel GT, Maceyka M, Milstien S, et al. Targeting the sphingosine-1-phosphate axis in cancer, inflammation and beyond. *Nat Rev Drug Discov*. 2013;12:688–702.
40. Karuppuchamy T, Behrens EH, González-Cabrera P, et al. Sphingosine-1-phosphate receptor-1 (S1P1) is expressed by lymphocytes, dendritic cells, and endothelium and modulated during inflammatory bowel disease. *Mucosal Immunol*. 2017;10:162–171.
41. McNamee EN, Masterson JC, Veny M, et al. Chemokine receptor CCR7 regulates the intestinal TH1/TH17/treg balance during Crohn's-like murine ileitis. *J Leukoc Biol*. 2015;97:1011–1022.
42. McNamee EN, Masterson JC, Jedlicka P, et al. Ectopic lymphoid tissue alters the chemokine gradient, increases lymphocyte retention and exacerbates murine ileitis. *Gut*. 2013;62:53–62.
43. Apostolaki M, Manoloukos M, Roulis M, et al. Role of beta7 integrin and the chemokine/chemokine receptor pair CCL25/CCR9 in modeled TNF-dependent Crohn's disease. *Gastroenterology*. 2008;134:2025–2035.
44. Rivera-Nieves J, Olson T, Bamias G, et al. L-selectin, alpha 4 beta 1, and alpha 4 beta 7 integrins participate in CD4+ T cell recruitment to chronically inflamed small intestine. *J Immunol*. 2005;174:2343–2352.
45. Maynard CL, Weaver CT. Intestinal effector T cells in health and disease. *Immunity*. 2009;31:389–400.
46. Bendall SC, Simonds EF, Qiu P, et al. Single-cell mass cytometry of differential immune and drug responses across a human hematopoietic continuum. *Science*. 2011;332:687–696.
47. Isoyama N, Takai K, Tsuchida M, et al. Evidence that FTY720 induces rat thymocyte apoptosis. *Transpl Immunol*. 2006;15:265–271.
48. Van Brocklyn JR, Williams JB. The control of the balance between ceramide and sphingosine-1-phosphate by sphingosine kinase: oxidative stress and the seesaw of cell survival and death. *Comp Biochem Physiol B Biochem Mol Biol*. 2012;163:26–36.
49. Matsumura M, Tsuchida M, Isoyama N, et al. FTY720 mediates cytochrome c release from mitochondria during rat thymocyte apoptosis. *Transpl Immunol*. 2010;23:174–179.
50. Maeda Y, Yagi H, Takemoto K, et al. S1P lyase in thymic perivascular spaces promotes egress of mature thymocytes via up-regulation of S1P receptor 1. *Int Immunol*. 2014;26:245–255.